World Journal of Gastroenterology

Online Submissions: http://www.wjgnet.com/1007-9327office
wjg@wjgnet.com
doi:10.3748/wjg.v16.i2.201

*World J Gastroenterol* 2010 January 14; 16(2): 201-209
ISSN 1007-9327 (print)


ORIGINAL ARTICLE

# Rupintrivir is a promising candidate for treating severe cases of Enterovirus-71 infection

Xiao-Nan Zhang, Zhi-Gang Song, Ting Jiang, Bi-Sheng Shi, Yun-Wen Hu, Zheng-Hong Yuan

Xiao-Nan Zhang, Zhi-Gang Song, Ting Jiang, Yun-Wen Hu, Zheng-Hong Yuan, Research Unit, Shanghai Public Health Clinical Center, Caolang Road 2901, Shanghai 201508, China
Bi-Sheng Shi, Zheng-Hong Yuan, Key Laboratory of Medical Molecular Virology, Shanghai Medical College, Fudan University Dongan Road 130, Shanghai 200032, China
Author contributions: Zhang XN performed the majority of experiments and molecular simulations; Song ZG provided cDNA samples of EV71 infected patients; Jiang T performed phylogenetic analyses; Shi BS performed the cloning and sequencing of EV71 3C protease fragments; Hu YW and Yuan ZH coordinated and helped design the project.
Supported by Start-up Fund (No. KSF0062) of the Shanghai Public Health Clinical Center
Correspondence to: Zheng-Hong Yuan, Professor, Research Unit, Shanghai Public Health Clinical Center, Caolang Road 2901, Shanghai 201508, China. zhyuan@shaphc.org
Telephone: +86-21-64161928 Fax: +86-21-64227201
Received: October 7, 2009 Revised: November 8, 2009
Accepted: November 15, 2009
Published online: January 14, 2010

## Abstract

**AIM:** To evaluate the suitability of rupintrivir against Enterovirus 71 (EV71) induced severe clinical symptoms using computational methods.

**METHODS:** The structure of EV71 3C protease was predicted by homology modeling. The binding free energies between rupintrivir and EV71 3C and human rhinovirus 3C protease were computed by molecular dynamics and molecular mechanics Poisson-Boltzmann/surface area and molecular mechanics generalized-born/surface area methods. EV71 3C fragments obtained from clinical samples collected during May to July 2008 in Shanghai were amplified by reverse-transcription and polymerase chain reaction and sequenced.

**RESULTS:** We observed that rupintrivir had favorable binding affinity with EV71 3C protease (-10.76 kcal/mol). The variability of the 3C protein sequence in isolates of various outbreaks, including those obtained in our hospital from May to July 2008, were also analyzed to validate the conservation of the drug binding pocket.

**CONCLUSION:** Rupintrivir, whose safety profiles had been proved, is an attractive candidate and can be quickly utilized for treating severe EV71 infection.



**Key words:** Rupintrivir; Hand foot and mouth disease; Molecular mechanics Poisson-Boltzmann/surface area; Molecular mechanics Generalized-Born/surface area; Homology modeling; Picornavirus

**Peer reviewers:** Dr. Akhilesh B Reddy, MD, PhD, Institute of Metabolic Science, Level 4, Addenbrooke's Hospital (ATC), Box 289, Cambridge, CB2 0QQ, United Kingdom; Alain L Servin, PhD, Faculty of Pharmacy, French National Institute of Health and Medical Research, Unit 756, Rue J.-B. Clément, F-922296 Châtenay-Malabry, France

Zhang XN, Song ZG, Jiang T, Shi BS, Hu YW, Yuan ZH. Rupintrivir is a promising candidate for treating severe cases of Enterovirus-71 infection. *World J Gastroenterol* 2010; 16(2): 201-209 Available from: URL: http://www.wjgnet.com/1007-9327/full/v16/i2/201.htm DOI: http://dx.doi.org/10.3748/wjg.v16.i2.201

## INTRODUCTION

During March to May 2008, an outbreak of hand, foot and mouth disease (HFMD) erupted in Anhui province, China. Thousands of people, mostly infants and children, were admitted into hospitals with moderate to severe symptoms, e.g. encephalitis, aseptic meningitis and pulmonary edema *etc.*, and over twenty deaths were reported by the health authorities. Laboratory investigations revealed that human enterovirus 71 (EV71) was responsible for this epidemic. Our center also

received 103 cases of HFMD (77 positive for EV71) from May to July 2008 with mild (fever, pneumonia) to severe (meningitis, encephalitis) symptoms and one patient died of viral encephalitis. Currently, treatment options for EV71 infection are limited, individual symptoms such as fever, encephalitis and meningitis are eased by supportive medication.

EV71 belongs to the picornaviridae family, which also include Poliovirus, Rhinovirus, and Coxsackie virus *etc*. It has a 7.4 kb positive-stranded RNA genome encoding one big polyprotein which was cleaved by virally encoded 2A and 3C protease in the process of protein synthesis[1]. This results in four structural proteins, VP1, VP2, VP3, VP4, and several non-structural proteins, 2A, 2B, 2C, 3A, 3B, 3C and 3D-Pol. In addition to its role in precursor polyprotein cleavage, the 3C protease is capable of cleaving host factors associated with host cell transcription and binding viral RNA as a constituent of replication complex[2-4]. The pivotal role of 3C in the viral life cycle makes it an ideal target for drug design. Indeed, there have been publications on the development of 3C peptidomimetic inhibitors against the picornaviridae family members[5-7], including HRV (Human rhinovirus), an etiological cause of common colds[8]. Among them, rupintrivir (Figure 1), an irreversible inhibitor of HRV 3C, is by far the only 3C inhibitor that has entered clinical trials[9-12]. Matthews *et al*[8] designed this molecule by taking advantage of covalent adduct formation (Michael reaction) with a reactive serine or cysteine at the active site of the protease such that the inhibitory potency is greatly enhanced. The Phase I and Phase Ⅱ results, according the company's press release, showed good safety and pharmacokinetics profiles. Furthermore, reduction in respiratory symptom scores and HRV titer in the upper respiratory tract of experimentally induced HRV infection was also documented.

It has been recently reported that a cell based yeast two hybrid assay system supported the idea that rupintrivir can effectively bind to EV71 3C[13]. We attempted to evaluate the affinity of rupintrivir to EV71 3C by homology modeling and atomistic molecular dynamics (MD) simulation. First, a comparative model of EV71 3C was constructed based on the crystal structure of HRV (1CQQ) and Poliovirus 3C protease (1L1N). EV71 3C-rupintrivir was then modeled according to the HRV 3C-rupintrivir complex (1CQQ) and 2 nanosecond MD simulations were performed on both complexes. We observed that rupintrivir can fit into the catalytic core of EV71 3C and is stable during MD. Binding free energy analyses using molecular mechanics Poisson-Boltzmann/surface area and molecular mechanics generalized-born/surface area methods were also performed. The estimated values suggested that rupintrivir has a decreased but still favorable affinity to EV71 3C compared with its HRV homolog. To test whether rupintrivir could fit for the majority of circulating isolates of EV71, we collected the 3C sequences of various epidemics from Genbank together with those obtained from clinical isolates in our center and analyzed the effects on drug-target interaction. It was found that the residues which make direct contacts with rupintrivir showed minimal sequence variation in 48 divergent isolate sequences. Taken together, we suggest that rupintrivir has a significant affinity and chemical reaction rate with EV71 3C. Given that the pharmacokinetics and safety profiles of this drug have been proved, the findings of this study suggest that rupintrivir may be speedily utilized for treatment of severe EV71 infections, which will be significantly more efficient, in terms of time and resource, than development from a new chemical entity.

## MATERIALS AND METHODS

### Patients

One hundred and three cases of HFMD were admitted into the Shanghai Public Health Clinical Center and tested for EV71 and Coxsackie virus 16 with reverse transcription and polymerase chain reaction during May to July 2008. Seventy seven of these patients tested positive for EV71, in whom, respiratory symptoms and neurological symptoms (meningitis, encephalitis) were documented. There was one death of a 20-mo-old child caused by severe viral encephalitis after being transferred to our hospital.

### Viral culture, sequencing and phylogenetic analysis

Throat swabs and stools were obtained from patients with HFMD in Shanghai public health clinical center. If they tested positive for EV71, samples were grown in RD cells, a human rhabdomyosarcoma cell line, in DMEM with 10% fetal bovine serum, 2 mmol/mL L-glutamine, 100 U/mL penicillin and 0.1 mg/mL streptomycin at 37℃ with 5% $CO_2$. If cytopathic effects were observed, culture supernatants were collected and RNA was extracted with TRIzol (Invitrogen) reagent and reverse transcribed with superscript Ⅱ reverse transcriptase (Invitrogen). cDNA from four isolates (42T, 44T, 61T, 122F) were used as templates to amplify viral 3C sequence. The primers used were as follows, 3C forward: 5'-GATYRTHCCTGAW RCTCCCACCA, 3C reverse 5'-GGGTCTTTACTRKK CAASACWG. The 891 bp fragment covering the entire 3C sequence was amplified and TA-cloned into pGEM-T easy vector (Promega). To ensure accuracy, each cDNA was amplified and TA-cloned twice and each clone was sequenced in both directions and assembled. Nucleotide sequences of the 3C region of the four EV71 strains were submitted to Genbank and were analyzed together with the 44 strains in GenBank. The 48 strains were aligned with CLUSTALX software. Phylogenetic trees were constructed by the neighbor joining method and plotted using the program Tree-view. The robustness of the trees was then tested by bootstrap analysis with 1000 pseudo-replicates.

### Homology modeling of EV71 3C protease

The 3C reference sequence (GenBank EU703812) was from a complete genome of an EV71 isolate in Fuyang, Anhui Province, May 2008 and was reported by National

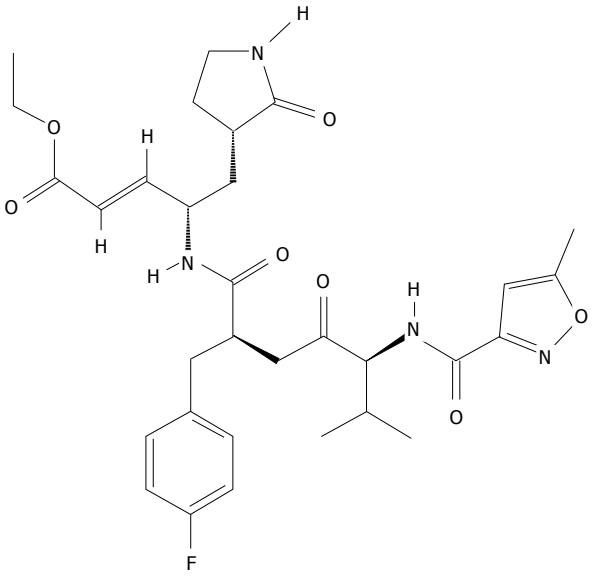

**Figure 1 Chemical structure of rupintrivir.**

Polio and Measles Lab, Institute for Viral Disease Control and Prevention, China CDC. Two homologous entries in the protein data bank with over 44% and 55% identity, i.e. 1CQQ (HRV 3C-rupintrivir complex, resolution 1.85 Å) and 1L1N (poliovirus 3C, resolution 2.10 Å) were used as templates for modeling. Homology modeling was performed on a SGI Tezro workstation using the *Homology* module in the Insight Ⅱ 2000 software package. The protein sequences were aligned with PSI-BLAST and were further refined by using structural alignment functionality. This alignment was used for comparative modeling implemented in the *Modeler* module which generates structures by applying spatial restraints and MD refinement[14]. Three models were generated with the optimization level set as "high" and the coordinate with the lowest probability density function value was chosen. The quality of the model was assessed by *MolProbity* sever[15] and 3*D-profile*[16,17].

The initial coordinate for the EV71 3C-rupintrivir complex was constructed in Insight Ⅱ according to the 1CQQ crystal structure. Briefly, EV71 3C and 1CQQ were superimposed and the covalent bond between the Cys147 thiol group and rupintrivir C19 was broken. After removal of HRV 3C protease, EV71 3C and rupintrivir were merged and subjected to further energy minimization.

### Molecular dynamic simulations

The simulations were performed using the AMBER 9 package with AMBER99SB[18] and GAFF[19] force fields. The coordinate of rupintrivir was prepared by breaking the bond between the inhibitor and the Cys147 thiol group in 1CQQ and resuming the trans-unsaturated bond. Partial charges and missing force field parameters were generated by the Antechamber program[19] in the AMBER suite using the AM1-BCC method. The 1CQQ complex (inhibitor detached from Cys147) and the EV71 3C-rupintrivir structure as described above were employed as the starting point for energy minimization and MD simulations. Missing hydrogen atoms were added using the Xleap program. The protonation state of the histidine residues was checked by H++ server[20]. The complexes were solvated with 8 Å of TIP3P in a truncated octahedron by *solvateOct* command in Xleap. The systems were neutralized by sodium or chlorine ions.

Because of the large VDW repulsion energy caused by the manually built coordinate, the EV71-rupintrivir complex was carefully minimized before starting MD in a four-step manner, with 200 cycles of steepest descent and 800 cycles of conjugate gradient each step and descending restraints (500, 50, 10 and 2 kcal/mol-Å$^2$). The 1CQQ complex was minimized with similar parameters except with less restraint (50, 10, 2 and 0 kcal/mol-Å$^2$). The particle mesh Ewald method was used to treat long-range electrostatics and a cutoff was set to 12 Å. The SHAKE procedure was utilized to fix all hydrogen atoms, the time step was set to 2.0 fs. The system was heated in 50 ps from 0 to 300 K using Langevin dynamics with a collision frequency of 2.0/ps and 2.0 kcal/mol-Å$^2$ restraint. A 500 ps equilibration was performed in a NPT ensemble followed by a 2 ns production dynamics. The coordinates were saved every 2 ps.

### Binding free energy analysis

The binding free energy was calculated using the MMPB-SA[21] and MMGB-SA procedures[22,23]. The binding free energy is calculated as follows: $\Delta G_{binding} = \Delta E_{gas} + \Delta G_{sol} - T\Delta S$, where $\Delta E_{gas} = \Delta E_{ele} + \Delta E_{vdw}$. The gas phase energy, desolvation energy and entropic contributions are averaged over the snapshots generated during MD. The desolvation energy can be further separated into polar and nonpolar parts, that is, $\Delta G_{sol} = \Delta G_{PB}/\Delta G_{GB} + \Delta G_{SA}$. The polar solvation energy can be estimated by Poisson Boltzmann or Generalized Born method implemented in the mm_pbsa script[23] in AMBER9. The nonpolar solvation energy ($\Delta G_{SA}$) is computed with Molsurf. The $\Delta G_{PB}$ was calculated with grid spacing set to 0.5 Å and ionic strength was set to 0. The $\Delta E_{gas}$ and $\Delta G_{sol}$ was calculated with 100 snapshots of the trajectory at time interval of 20 ps. The entropy contribution ($T\Delta S$) was estimated by normal-mode analysis utilizing the *nmode* module, which computes vibrational, rotational, and translational entropies. Each snapshot was minimized 50000 steps until the energy gradient was below 0.0001 kcal/mol Å with a distance-dependent dielectric constant of 4r (r is the distance between two atoms). Ten snapshots at each trajectory were calculated due to the computation cost of normal mode analysis.

### Energy decomposition using MM-GBSA method

Apart from the computation efficiency compared with the PBSA approach, the GBSA energies can be further decomposed on a per residue and even a backbone or side-chain basis which provides a simple means to evaluate energy contributions of each residue. All energy

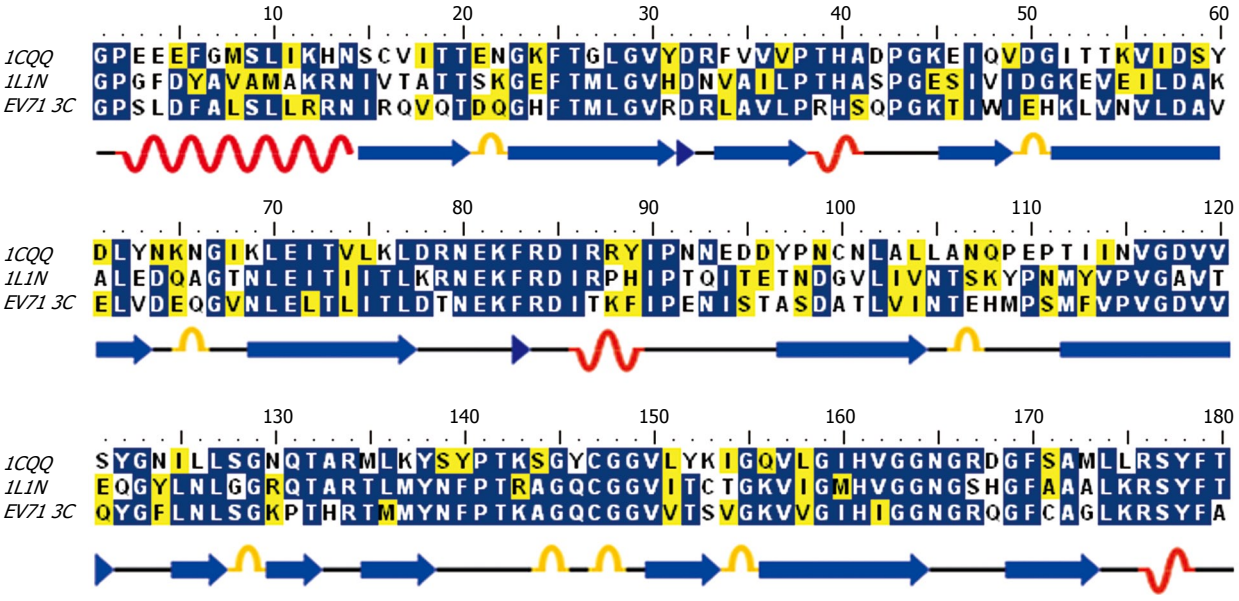


**Figure 2 Sequence alignment of EV71 3C protease with HRV 3C (1CQQ) and Poliovirus 3C (1L1N).** Secondary structures (α helixes and β sheets) were illustrated.

components were estimated using the decomposition functionality in *mm_pbsa* module using 100 snapshots of the trajectory at time interval of 20 ps.

### *Trajectory analysis and visualization*

Trajectories from MD simulation were analyzed by the *ptraj* module. Hydrogen bond formation was analyzed by the *hbond* command and atom-to-atom distance, angle and dihedral angle were measured by *distance, angle* and *dihedral* command, respectively. Trajectories were visualized and inspected by VMD[24], the Chimera suite[25] was used for graphic presentations of the complexes.

## RESULTS

### *Homology modeling of EV71 3C protease*

Using PSI-BLAST to search similar PDB sequences, a number of homologous entries were found including 1L1N (poliovirus 3C protease, 55% identity), 2IJD (poliovirus 3CD precursor, 54% identity), 2B0F (NMR structure of HRV 3C protease, 49% identity) and 1CQQ (Type 2 HRV 3C with rupintrivir, 44% identity). 1L1N[26] and 1CQQ[8] were subsequently chosen for template of homology modeling because of higher resolution and the preferable holo coordinate (Figure 2). The predicted structures generated by *Modeler* were then evaluated by *Profile-3D*; one model was selected with a score of 85.38 (expected score 82.94) and a sound folding profile for further analysis. The stereochemical property as indicated by the Ramachandran plot was highly reasonable. 98.9% of the residues were in favored regions and 99.4% were in allowed regions. Only one residue (Asp32) was barely outside of the allowed regions (data not shown).

The structure of EV71 3C protease retained the key features of HRV and poliovirus 3C with a two β-barrels fold and a shallow groove for substrate binding between

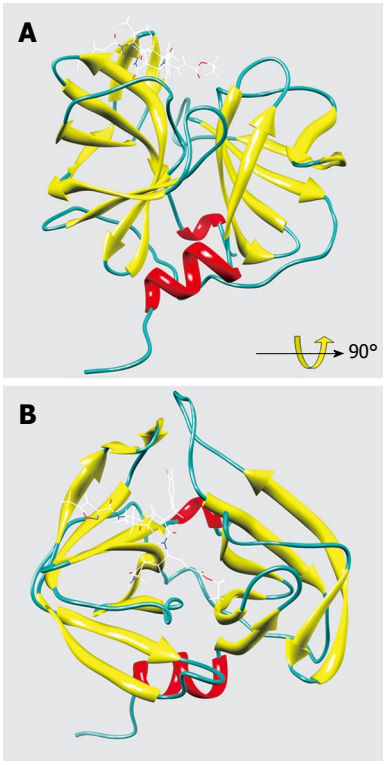


**Figure 3 The overall structure of EV71 3C protease complexed with rupintrivir.** A: A solid ribbon presentation of EV71 3C with rupintrivir; B: 90° rotation view of the structure.

the two domains (Figure 3). The backbone root mean square deviation (RMSD) between EV71 3C-1L1N and EV71 3C-1CQQ is 0.229 Å and 1.48 Å, respectively

### *Stability of the EV71 3C-rupintrivir complex*

To further probe the stability of the EV71 3C-rupintrivir complex, we then performed MD simulations and RMSD of $C_\alpha$ atoms during the production phase relative to initial coordinate was plotted (Figure 4A). Compared with 1CQQ complex (RMSD 1.04 Å), the EV71 protein backbone showed relatively higher displacement during

**Table 1 Binding free energies (kcal/mol) of Rhinovirus 3C protease and EV71 3C protease complexed with rupintrivir**

| Receptor | | $\Delta E_{ele}$ | $\Delta E_{vdw}$ | $\Delta G_{SA}$ | $\Delta G_{PB}$ | $\Delta G_{GB}$ | $-T\Delta S$ | $\Delta G_{PBSA}$ | $\Delta G_{GBSA}$ |
|---|---|---|---|---|---|---|---|---|---|
| Rhino 3C | Mean | -40.70 | -64.31 | -8.22 | 64.17 | 55.67 | 30.10 | -18.96 | -27.56 |
| | STD | 4.75 | 3.63 | 0.37 | 3.78 | 3.71 | 6.26 | 9.45 | 9.42 |
| EV71 3C | Mean | -37.74 | -60.67 | -8.11 | 66.68 | 56.24 | 28.87 | -10.76 | -21.41 |
| | STD | 8.57 | 3.75 | 0.16 | 5.88 | 5.23 | 3.85 | 11.70 | 11.39 |

$\Delta E_{ele}$: Coulombic energy; $\Delta E_{vdw}$: Van der Waals energy; $\Delta G_{SA}$: non-polar salvation free energy; $\Delta G_{PB}$: Poisson-Boltzmann polar solvation energy; $\Delta G_{GB}$: Generalized-Born polar salvation energy; $\Delta G_{PBSA} = \Delta E_{ele} + \Delta E_{vdw} + \Delta G_{SA} + \Delta G_{PB} - T\Delta S$; $\Delta G_{GBSA} = \Delta E_{ele} + \Delta E_{vdw} + \Delta G_{SA} + \Delta G_{GB} - T\Delta S$; STD: Standard error of mean values.

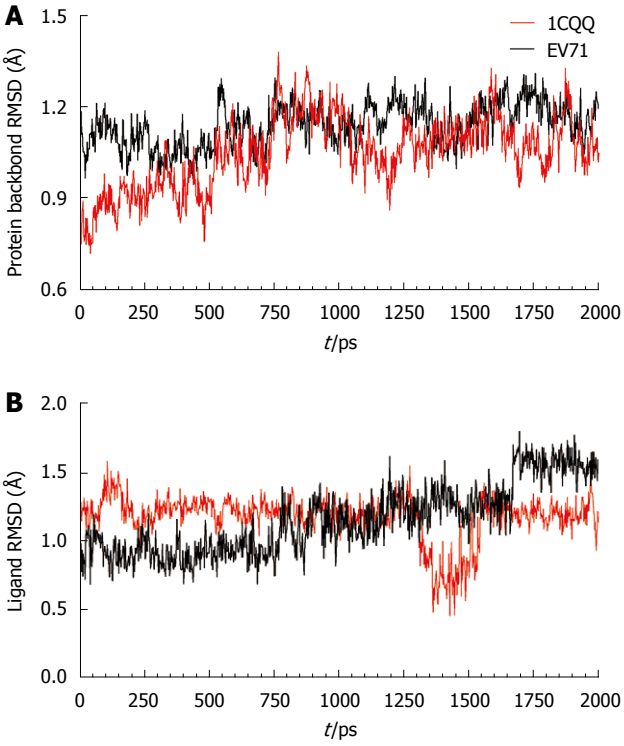


**Figure 4 Receptor and ligand backbone displacement.** A: Backbone root mean square deviation (RMSD) of the HRV 3C (1CQQ) and EV71 3C protein; B: Ligand backbone RMSD during the 2ns molecular dynamics simulation.

production MD (1.56 Å), which was mainly caused by the five N terminal residues ($G_1$PSLD$_5$). Unlike its template, 1CQQ, these residues didnot adopt a helical conformation and showed very high fluctuation during MD (data not shown). This was presumably caused by the less reasonable starting coordinate assigned during homology modeling. Nevertheless, these residues were not in close contact with the inhibitor and hence didnot significantly influence the binding energy. Indeed, if the displacement was measured without these residues, EV71 complex showed displacement similar to that of 1CQQ and reached equilibrium and remained stable during the simulation (Figure 4A). Ligand heavy-atom RMSD plot (Figure 4B) also indicated similar displacement (average, 1CQQ:1.18 Å, EV71: 1.16 Å) but remained stable in a 2ns run (STD, standard deviation, 1CQQ: 0.16 Å, EV71: 0.25 Å).

Both 1CQQ and EV71 MD simulations retained

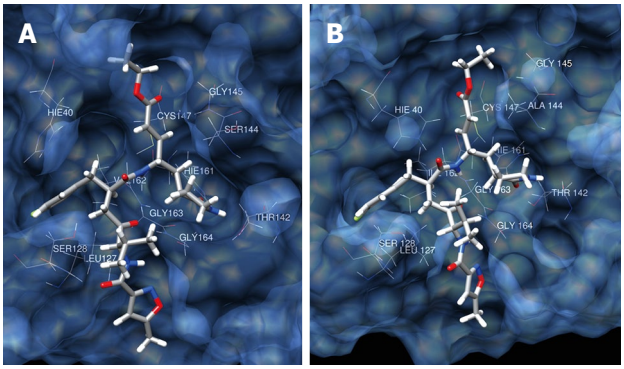


**Figure 5 Binding mode of AG7088 with 1CQQ (A) and EV71 3C (B).** The protein surface is rendered semitransparent with associated backbone and side chain atom.

the major binding mode in the crystal structure (Figure 5). The P1 lactam group filled into the pocket formed by Thr142, His 161 *etc*., the carboxamide oxygen and the amide nitrogen interacted with these residues *via* hydrogen bonds. The P2 4-fluoro-Phe group fitted very well in the S2 specificity pocket. The isoxazole group was buried in the S4 pocket and the vinyl group was close to and oriented well with the SG atom of Cys147.

### *Binding free energy estimate of EV71-rupintrivir complex*

We then estimated the binding free energy of EV71 complex and 1CQQ complex using MM-PBSA and MM-GBSA methods. To save computational cost, the singe trajectory approach was used since no significant conformational changes upon complex formation were reported. Indeed, 1L1N (no inhibitor bound) and 1CQQ (rupintrivir bound) have 0.75 Å backbone RMSD with 43.89% sequence identity, and the shapes of catalytic core are essentially the same (catalytic pocket residue backbone RMSD = 1.01 Å). As shown in Table 1, the PBSA method predicted binding free energy of -18.96 kcal/mol for 1CQQ and -10.76 for EV71 complex. However, the GBSA method gave considerably higher free energy (-27.56 kcal/mol for 1CQQ, -21.41 kcal/mol for EV71) because of lower estimation of unfavorable electrostatic solvation energy. The non-polar solvation energy gave a favorable contribution (-8.22 kcal/mol in 1CQQ and -8.11 kcal/mol in EV71) because of reduced surface area. Overall, we observed that the EV71 complex still had

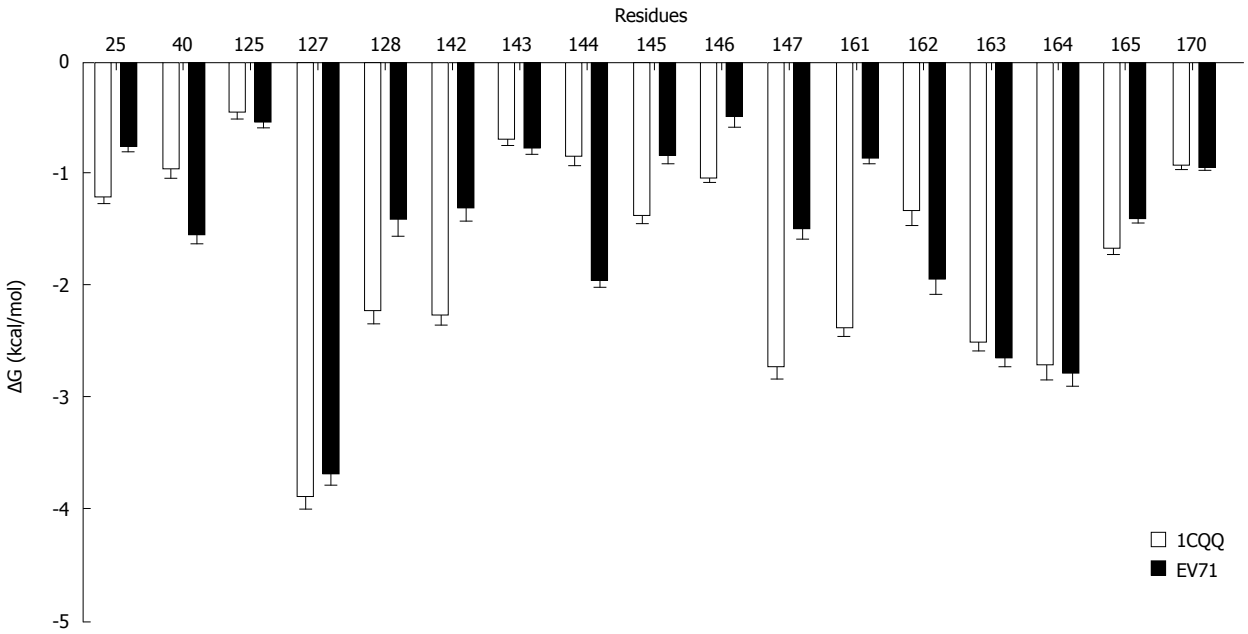


**Figure 6 Energy decomposition (using MM-GBSA) of the key interaction residues in 1CQQ and EV71 3C complexes.**

favorable binding energy although slightly lower than that in 1CQQ.

### *Energy decomposition*

To further analyze the energy contributions of individual residues, we decomposed the binding energies of 1CQQ and EV71 complex (Figure 6). It can be concluded from the plot that the decreased binding free energy was not governed by a single or two residues but a sum of cumulative effects. Indeed, residue Phe25, Ser128, Thr142, Gly145, 146Tyr/Gln, Cys147, His161 contributed less favorably in EV71 complex. Notably, all these sites, except for residue 146, have the same amino acid which suggests that the decreased energy contribution is caused by minute differences in the backbone coordinate. Nevertheless, we also observed several sites (His40, Ala144 and Ile162) that had more binding energy contributions than those in 1CQQ. Further analysis indicates that these residues all have preferred VDW and solvation energy.

### *Sequence variability of EV71 3C protease and its effect on rupintrivir binding*

As RNA viruses typically exhibit a high mutation rate in their replication process which could facilitate drug resistance, we sought to evaluate natural sequence variations in isolates collected in various epidemics and their effect on rupintrivir binding. Four sequences of 3C isolated in our hospital were also included (Figure 7A). Phylogeny analysis indicated that very high similarity between isolates in Shanghai and in Fuyang, Anhui province and 122F has 100% identity with the EU703812 reference sequence (Figure 7A). We then further scrutinized the variability of the residues with considerable contact with rupintrivir. As shown in Figure 8, most strains exhibited high conservation on key residues (red open box) in the binding site (residue 25, 40, 125-128, 142-147, 161-165, 170). However, variations on key sites were repeatedly shown in isolate 2272.TW.98 which was obtained from a patient who died of pulmonary hemorrhage and shock in 1998, Taiwan. Further structural analysis suggests that Arg128 in 2272.TW.98 (Ser in Reference sequence) may create a steric hindrance to the 4-fluoroPhe group of rupintrivir (Figure 7B). In addition, the Pro142 in 2086.TW.98, which replaced the conserved Thr residue important for hydrogen bond formation with the lactam ring, could also drastically affect inhibitor docking. The variability observed in residue 144, 145 in 2272.TW.98 and BrCr.70 is unlikely to abolish rupintrivir's activity as the unsaturated ester group is shown to be quite flexible in simulation (data not shown). Taken together, although the catalytic core of EV71 3C is generally preserved in a wide range of isolates, potential natural drug resistance may exist which would limit the usefulness of rupintrivir.

## DISCUSSION

Since the first case of EV71 infection in California in 1969, EV71 has been identified in several small-scale outbreaks in United States, Europe, Australia, Japan, Brazil and Malaysia[27-32]. EV71 infection has become a prominent public health issue since the outbreak in Taiwan, China, 1998, with 129 106 cases of HFMD and 405 cases of severe disease[33]. Notably, a recent EV71 epidemic in Anhui province during March to May 2008, PR China has also caused over 20 deaths and raised public awareness of the HFMD.

There have been some reports on anti-EV71 drug development in recent years[34-36]. Notably, Kuo *et al*[7] designed a series of compounds against EV71 3C based on the structure of rupintrivir. Nevertheless, most of these drugs are still in the early phase and need

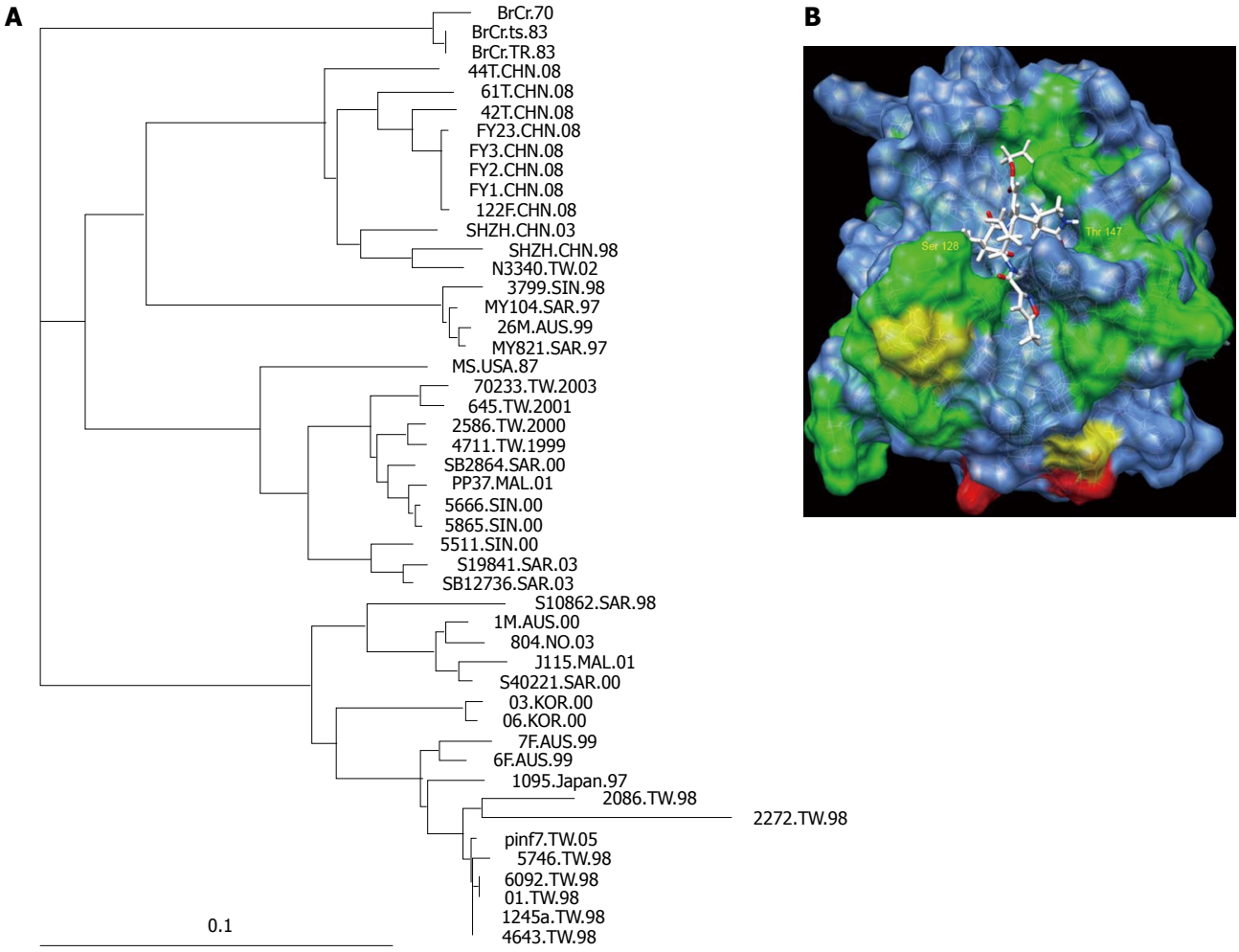


**Figure 7 Sequence variability of EV71 3C protease and its effect on rupintrivir binding.** A: Phylogenetic tree of 48 isolates of EV71 in various outbreaks; B: A colored representation of sequence variation on the surface of 3C protease. Positions with two, three and over three different residues are labeled green, yellow and red, respectively. Residue Ser 128 and Thr 142 were labeled.

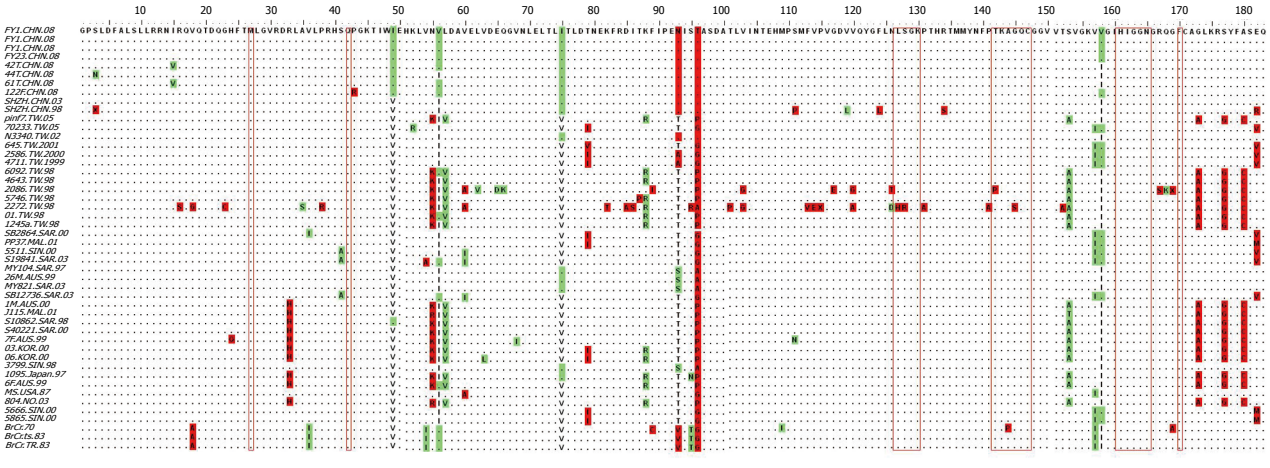


**Figure 8 Sequence alignment of 3C protease from isolates collected in various epidemics (CHN: Mainland China; TW: Taiwan, China; FY: Fuyang, Anhui Province, China; SHZN: Shenzhen, China; AUS: Australia; SAR, SIN, MAL: Malaysia; KOR: Korea; NO: Norway).** Residues important for rupintrivir are labeled with red open boxes.

further optimization of pharmacokinetics and ADMET (absorption, distribution, metabolism, excretion and toxicity) profiles. EV71 vaccine research is also in an early development stage[37] and needs further human safety tests. The scarcity of available antiviral medication renders clinical intervention of severe cases challenging.

In this report, we suggest that an available drug, rupintrivir, is an attractive candidate for treatment of

severe cases of EV71 infection. MD and MM-PBSA (GBSA) analysis suggested a decreased but still favorable interaction with EV71 3C protease compared with HRV 3C. In addition, rupintrivir had been shown to be effective against all the human HRV serotypes and several human enterovirus strains (CVB2, 5, EV6, 9) because of high conservation in the rupintrivir binding site, although EV71 was not tested[9]. Recently, using plaque reduction assay and a real-time fluorescence resonance energy transfer model, rupintrivir showed around 0.8 μmol/L EC50 activity[38]. Of note, the EC50 in EV71 (0.8 μmol/L[38]) and in type 2 HRV (20 nmol/L[8,9]) can be well correlated with free energy estimate in our research (-18.96 kcal/mol in HRV and -10.76 kcal/mol in EV71, MM-PBSA method). Collectively, using molecular simulation and binding free energy estimation, we suggest that rupintrivir can effectively inhibit EV71 3C protease, which is confirmed by recent *in vitro* viral culture study. Utilization of old drugs for treatment of new indications has its intrinsic superiority since all the pre-clinical research and most of clinical research can be obviated. If rupintrivir could prove its efficacy in HFMD patients, this drug could be quickly administered to EV71 patients with severe symptoms and possibly reduce the mortality rate of HFMD in infants.

## COMMENTS

### Background

The enterovirus 71 (EV71) is the major pathogen causing hand foot and mouth disease (HFMD). During March to May 2008, an epidemic of HFMD erupted in Anhui province and the surrounding area, China with significant mortality. The authors' hospital received over one hundred of these patients including several with severe complications.

### Research frontiers

To date, there have been no antiviral drugs available for EV71 infection with severe symptoms. Although, reports of compounds that can inhibit EV71 replication *in vitro* are accumulating, they still need to be tested in pharmacokinetics, ADMET (absorption, distribution, metabolism, excretion and toxicity) and other safety profiles.

### Innovations and breakthroughs

In this article, the authors modeled the EV71 3C protease, which is critical for viral replication, based on the crystal structure of rhinovirus and poliovirus 3C. They further evaluated an irreversible inhibitor of rhinovirus 3C, rupintrivir as a possible drug against EV71 by molecular dynamics and molecular mechanics Poisson-Boltzmann/surface area and molecular mechanics generalized-born/surface area methods. This is the first attempt to computationally evaluate the suitability of rupintrivir in inhibiting EV71 3C protease.

### Applications

With the *in vitro* and computational evidence supporting its anti-EV71 activity together with its safety profile in previous clinical trials, rupintrivir may be quickly administered to EV71 patients with severe symptoms and possibly reduce the mortality rate of HFMD in infants.

### Terminology

EV71 belongs to the picornaviridae family and is the major cause of HFMD. HFMD is a human syndrome caused by intestinal viruses of the picornaviridae family. The most common viruses causing HFMD are Coxsackie A virus and EV71. HFMD usually affects infants and children and mostly causes mild symptoms. However, significant mortality has been observed in Anhui province 2008 and in previous outbreaks in Taiwan in 1998.

### Peer review

The manuscript is a predictive study for the use of rupintrivir against EV71 infection, based on a computer analysis of the relationship of rupintrivir structure and EV71 structure. Data showed the potential binding of rupintrivir on the EV71 3C protease. The study is well conducted and the analysis appears solid.

## REFERENCES


1 **Kräusslich HG**, Nicklin MJ, Lee CK, Wimmer E. Polyprotein processing in picornavirus replication. *Biochimie* 1988; **70**: 119-130

2 **Roehl HH**, Parsley TB, Ho TV, Semler BL. Processing of a cellular polypeptide by 3CD proteinase is required for poliovirus ribonucleoprotein complex formation. *J Virol* 1997; **71**: 578-585

3 **Leong LE**, Walker PA, Porter AG. Human rhinovirus-14 protease 3C (3Cpro) binds specifically to the 5'-noncoding region of the viral RNA. Evidence that 3Cpro has different domains for the RNA binding and proteolytic activities. *J Biol Chem* 1993; **268**: 25735-25739

4 **Xiang W**, Harris KS, Alexander L, Wimmer E. Interaction between the 5'-terminal cloverleaf and 3AB/3CDpro of poliovirus is essential for RNA replication. *J Virol* 1995; **69**: 3658-3667

5 **Lee ES**, Lee WG, Yun SH, Rho SH, Im I, Yang ST, Sellamuthu S, Lee YJ, Kwon SJ, Park OK, Jeon ES, Park WJ, Kim YC. Development of potent inhibitors of the coxsackievirus 3C protease. *Biochem Biophys Res Commun* 2007; **358**: 7-11

6 **Lall MS**, Jain RP, Vederas JC. Inhibitors of 3C cysteine proteinases from Picornaviridae. *Curr Top Med Chem* 2004; **4**: 1239-1253

7 **Kuo CJ**, Shie JJ, Fang JM, Yen GR, Hsu JT, Liu HG, Tseng SN, Chang SC, Lee CY, Shih SR, Liang PH. Design, synthesis, and evaluation of 3C protease inhibitors as anti-enterovirus 71 agents. *Bioorg Med Chem* 2008; **16**: 7388-7398

8 **Matthews DA**, Dragovich PS, Webber SE, Fuhrman SA, Patick AK, Zalman LS, Hendrickson TF, Love RA, Prins TJ, Marakovits JT, Zhou R, Tikhe J, Ford CE, Meador JW, Ferre RA, Brown EL, Binford SL, Brothers MA, DeLisle DM, Worland ST. Structure-assisted design of mechanism-based irreversible inhibitors of human rhinovirus 3C protease with potent antiviral activity against multiple rhinovirus serotypes. *Proc Natl Acad Sci USA* 1999; **96**: 11000-11007

9 **Binford SL**, Maldonado F, Brothers MA, Weady PT, Zalman LS, Meador JW 3rd, Matthews DA, Patick AK. Conservation of amino acids in human rhinovirus 3C protease correlates with broad-spectrum antiviral activity of rupintrivir, a novel human rhinovirus 3C protease inhibitor. *Antimicrob Agents Chemother* 2005; **49**: 619-626

10 **Patick AK**. Rhinovirus chemotherapy. *Antiviral Res* 2006; **71**: 391-396

11 **Binford SL**, Weady PT, Maldonado F, Brothers MA, Matthews DA, Patick AK. In vitro resistance study of rupintrivir, a novel inhibitor of human rhinovirus 3C protease. *Antimicrob Agents Chemother* 2007; **51**: 4366-4373

12 **Patick AK**, Brothers MA, Maldonado F, Binford S, Maldonado O, Fuhrman S, Petersen A, Smith GJ 3rd, Zalman LS, Burns-Naas LA, Tran JQ. In vitro antiviral activity and single-dose pharmacokinetics in humans of a novel, orally bioavailable inhibitor of human rhinovirus 3C protease. *Antimicrob Agents Chemother* 2005; **49**: 2267-2275

13 **Lee JC**, Shih SR, Chang TY, Tseng HY, Shih YF, Yen KJ, Chen WC, Shie JJ, Fang JM, Liang PH, Chao YS, Hsu JT. A mammalian cell-based reverse two-hybrid system for functional analysis of 3C viral protease of human enterovirus 71. *Anal Biochem* 2008; **375**: 115-123

14 **Sali A**, Blundell TL. Comparative protein modelling by satisfaction of spatial restraints. *J Mol Biol* 1993; **234**: 779-815

15 **Davis IW**, Leaver-Fay A, Chen VB, Block JN, Kapral GJ, Wang X, Murray LW, Arendall WB 3rd, Snoeyink J, Richardson JS, Richardson DC. MolProbity: all-atom contacts and structure validation for proteins and nucleic acids. *Nucleic Acids Res* 2007; **35**: W375-W383

16 **Bowie JU**, Lüthy R, Eisenberg D. A method to identify protein sequences that fold into a known three-dimensional structure. *Science* 1991; **253**: 164-170
17 **Lüthy R**, Bowie JU, Eisenberg D. Assessment of protein models with three-dimensional profiles. *Nature* 1992; **356**: 83-85
18 **Hornak V**, Abel R, Okur A, Strockbine B, Roitberg A, Simmerling C. Comparison of multiple Amber force fields and development of improved protein backbone parameters. *Proteins* 2006; **65**: 712-725
19 **Wang J**, Wolf RM, Caldwell JW, Kollman PA, Case DA. Development and testing of a general amber force field. *J Comput Chem* 2004; **25**: 1157-1174
20 **Gordon JC**, Myers JB, Folta T, Shoja V, Heath LS, Onufriev A. H++: a server for estimating pKas and adding missing hydrogens to macromolecules. *Nucleic Acids Res* 2005; **33**: W368-W371
21 **Srinivasan J**, Miller J, Kollman PA, Case DA. Continuum solvent studies of the stability of RNA hairpin loops and helices. *J Biomol Struct Dyn* 1998; **16**: 671-682
22 **Gohlke H**, Case DA. Converging free energy estimates: MM-PB(GB)SA studies on the protein-protein complex Ras-Raf. *J Comput Chem* 2004; **25**: 238-250
23 **Gohlke H**, Kiel C, Case DA. Insights into protein-protein binding by binding free energy calculation and free energy decomposition for the Ras-Raf and Ras-RalGDS complexes. *J Mol Biol* 2003; **330**: 891-913
24 **Humphrey W**, Dalke A, Schulten K. VMD: visual molecular dynamics. *J Mol Graph* 1996; **14**: 33-38, 27-28
25 **Pettersen EF**, Goddard TD, Huang CC, Couch GS, Greenblatt DM, Meng EC, Ferrin TE. UCSF Chimera--a visualization system for exploratory research and analysis. *J Comput Chem* 2004; **25**: 1605-1612
26 **Mosimann SC**, Cherney MM, Sia S, Plotch S, James MN. Refined X-ray crystallographic structure of the poliovirus 3C gene product. *J Mol Biol* 1997; **273**: 1032-1047
27 **Blomberg J**, Lycke E, Ahlfors K, Johnsson T, Wolontis S, von Zeipel G. Letter: New enterovirus type associated with epidemic of aseptic meningitis and-or hand, foot, and mouth disease. *Lancet* 1974; **2**: 112
28 **Schmidt NJ**, Lennette EH, Ho HH. An apparently new enterovirus isolated from patients with disease of the central nervous system. *J Infect Dis* 1974; **129**: 304-309
29 **da Silva EE**, Winkler MT, Pallansch MA. Role of enterovirus 71 in acute flaccid paralysis after the eradication of poliovirus in Brazil. *Emerg Infect Dis* 1996; **2**: 231-233
30 **Gilbert GL**, Dickson KE, Waters MJ, Kennett ML, Land SA, Sneddon M. Outbreak of enterovirus 71 infection in Victoria, Australia, with a high incidence of neurologic involvement. *Pediatr Infect Dis J* 1988; **7**: 484-488
31 **Ishimaru Y**, Nakano S, Yamaoka K, Takami S. Outbreaks of hand, foot, and mouth disease by enterovirus 71. High incidence of complication disorders of central nervous system. *Arch Dis Child* 1980; **55**: 583-588
32 **Khetsuriani N**, Lamonte-Fowlkes A, Oberst S, Pallansch MA. Enterovirus surveillance--United States, 1970-2005. *MMWR Surveill Summ* 2006; **55**: 1-20
33 **Ho M**, Chen ER, Hsu KH, Twu SJ, Chen KT, Tsai SF, Wang JR, Shih SR. An epidemic of enterovirus 71 infection in Taiwan. Taiwan Enterovirus Epidemic Working Group. *N Engl J Med* 1999; **341**: 929-935
34 **Lin CW**, Wu CF, Hsiao NW, Chang CY, Li SW, Wan L, Lin YJ, Lin WY. Aloe-emodin is an interferon-inducing agent with antiviral activity against Japanese encephalitis virus and enterovirus 71. *Int J Antimicrob Agents* 2008; **32**: 355-359
35 **Chang JS**, Wang KC, Chiang LC. Sheng-Ma-Ge-Gen-Tang inhibited Enterovirus 71 infection in human foreskin fibroblast cell line. *J Ethnopharmacol* 2008; **119**: 104-108
36 **Arita M**, Wakita T, Shimizu H. Characterization of pharmacologically active compounds that inhibit poliovirus and enterovirus 71 infectivity. *J Gen Virol* 2008; **89**: 2518-2530
37 **Chung YC**, Ho MS, Wu JC, Chen WJ, Huang JH, Chou ST, Hu YC. Immunization with virus-like particles of enterovirus 71 elicits potent immune responses and protects mice against lethal challenge. *Vaccine* 2008; **26**: 1855-1862
38 **Tsai MT**, Cheng YH, Liu YN, Liao NC, Lu WW, Kung SH. Real-time monitoring of human enterovirus (HEV)-infected cells and anti-HEV 3C protease potency by fluorescence resonance energy transfer. *Antimicrob Agents Chemother* 2009; **53**: 748-755


**S- Editor** Wang JL **L- Editor** O'Neill M **E- Editor** Ma WH